Organic Electronics 13 (2012) 2401–2405

Contents lists available at SciVerse ScienceDirect

Organic Electronics

journal homepage: www.elsevier.com/locate/orgel

Mechanical bending of flexible complementary inverters based on organic and oxide thin film transistors

D.I. Kim [a], B.U. Hwang [a], J.S. Park [a], H.S. Jeon [a], B.S. Bae [c], H.J. Lee [a], N.-E. Lee [a,b,*]

[a] School of Advanced Materials Science & Engineering, Sungkyunkwan University, Suwon, Kyunggi-do 440-746, Republic of Korea
[b] SKKU Advanced Institute of Nano Technology (SAINT), Sungkyunkwan University, Suwon, Kyunggi-do 440-746, Republic of Korea
[c] Department of Semiconductor and Display Engineering, Hoseo University, Asan 336-795, Republic of Korea

ARTICLE INFO

Article history:
Received 20 April 2012
Received in revised form 27 June 2012
Accepted 28 June 2012
Available online 13 July 2012

Keywords:
Flexible circuits
Complementary inverters
Thin film transistors
Hybrid structure
Pentacene

ABSTRACT

Flexible complementary inverters composed of p-channel pentacene thin-film transistors (TFTs) and n-channel amorphous indium gallium zinc oxide TFTs were fabricated on polymer substrates. The characteristics of the TFTs and inverters were evaluated at different bending radii. Throughout the bending experiments, the relationship between the performances of the inverters and the characteristics of the TFTs under mechanical deformation was analyzed. The mechanically applied strain led to a change in the voltage transfer characteristics of the complementary inverters, as well as the source–drain saturation current, field-effect mobility and threshold voltage of the TFTs. The switching threshold voltage of the fabricated inverters decreased with decreasing bending radius, which was related to changes in the field-effect mobility and the threshold voltage of the TFTs.

1. Introduction

Complementary inverters based on thin-film transistors (TFTs) are important because they have low power consumption and high voltage gain compared to single type circuits [1–5]. For example, circuits composed of Si TFTs have been investigated for a long time [6–9]. However, there might be some limitations on their applications in the field of flexible electronics due to their high process temperature and rigidity, which means that a special structural design is required to minimize strain in the active layer of the TFT structure [9,10]. For the fabrication of complementary inverters on flexible substrates, the process temperature should be decreased as much as possible. In order to replace the Si TFTs, organic and oxide TFTs have been extensively studied. Organic TFTs have attracted much attention in a wide range of applications that require large-area and low-cost TFTs, such as flexible displays [11,12], radio-frequency identification (RFID) tags [13], and smart cards [14]. Among p-channel organic semiconductors, polycrystalline pentacene ($C_{22}H_{14}$) is one of the promising candidates due to its commercial availability, good electrical performance, high mechanical flexibility, and low process temperature [15–20]. On the other hand, n-channel organic semi-conductors have shown extremely low carrier mobility even under a high voltage bias [21,22].

In contrast to organic materials, most oxide semiconductors based on transition metal oxides (TMO) have n-type properties, which have several merits compared to amorphous or polycrystalline silicon. To provide good electrical characteristics, Si TFTs require a crystallization process such as high temperature annealing, while oxide TFTs can be formed at low temperatures because they have high carrier mobility even in the amorphous phase. In particular, amorphous indium gallium zinc oxide (IGZO) is one of the most widely investigated oxide semiconductors. Hence, hybrid complementary inverters based on organic and inorganic TFTs with good voltage transfer characteristics and high voltage gain in flexible applications have been recently reported [4,5]. In practice, however, research

* Corresponding author at: School of Advanced Materials Science & Engineering, Sungkyunkwan University, Suwon, Kyunggi-do 440-746, Republic of Korea.
E-mail address: nelee@skku.edu (N.-E. Lee).

1566-1199/$ - see front matter © 2012 Elsevier B.V. All rights reserved.
http://dx.doi.org/10.1016/j.orgel.2012.06.038

into the phenomena caused by the mechanical deformation of circuits has not been reported, even though mechanical deformation affects the operation characteristics of circuits. Even in single structural TFTs, some related phenomena such as changes in the output current, leakage current, and field-effect channel mobility were observed when the devices were mechanically bent. Therefore, an evaluation of the effect of strain on circuits together with the effect on TFTs is necessary.

In flexible electronics, the strain induced in the devices under mechanical deformation should be reduced as much as possible. Among the methods to minimize the strain induced during mechanical bending, one of the most popular approaches is to situate the active layer at the mechanical neutral plane position where the induced strain is zero [23]. Devices located near the mechanical neutral plane withstand mechanical deformation well even at an extremely small bending radius of 1 mm [23]. However, there might be limits on where the mechanical neutral plane can be situated in devices which have various different functions on a single large-area substrate. Since most of the devices consist of multiple layers, this approach may not be a complete solution. Therefore, a deep understanding of the relationship between each TFT and inverter is required in advance in order to design and manufacture flexible devices.

In this work, we carried out mechanical bending experiments on flexible hybrid complementary inverters based on organic and inorganic TFTs. The characteristics of TFTs and inverters were evaluated under mechanical deformation which causes a tensile strain. In these bending experiments, it was found that changes in the field-effect mobility and threshold voltage in the TFTs affect the voltage transfer characteristics of an inverter circuit.

2. Device fabrication and measurement method

Complementary inverters using pentacene and IGZO TFTs as the p-channel and n-channel TFTs, respectively, were fabricated on a 125-μm-thick flexible polyimide (PI) substrate, as shown in Fig. 1(a). First, the PI substrate was cleaned sequentially by acetone, alcohol, and de-ionized water with ultra-sonication, and then it was baked at 120 °C for 1 h on a hot plate to remove residual solvent and water. A cross-linked poly-4vinyl phenol (PVP) layer was spin coated on the PI substrate to produce a smooth surface with a root mean-squared roughness below 1 nm, which was required for the formation of a high quality active layer. Then, Ni was deposited as the common gate electrodes of both TFTs on the PVP layer by e-beam evaporation using metal shadow masks. For high flexibility under mechanical deformation, 400-nm-thick PVP was used as an organic gate dielectric layer, which was formed by spin coating and thermally annealed at 200 °C. Then, 70-nm-thick pentacene semiconductor layers and Au source/drain electrodes were deposited by thermal evaporation using shadow masks at 80 °C and room temperature, respectively.

After the fabrication of pentacene TFTs was completed, they were encapsulated by plasma-polymerized methylcyclohexane (*pp*-MCH) and Al_2O_3 layers, which were deposited by plasma-enhanced chemical vapor deposition and atomic-layer deposition, respectively. In particular, the Al_2O_3 layer plays an important role during the fabrication of n-channel TFTs by preventing sputtering damage to organic TFTs during the deposition of an inorganic active layer. A 70-nm-thick IGZO layer (In_2O_3:Ga_2O_3:ZnO = 1:1:1 mol%) was deposited by RF sputtering under optimized conditions, including a power of 100 W and a working pressure of 5 mTorr in a mixture of 1% O_2/($Ar + O_2$) at room temperature. Finally, Al source/drain electrodes were deposited by thermal evaporation using a shadow mask.

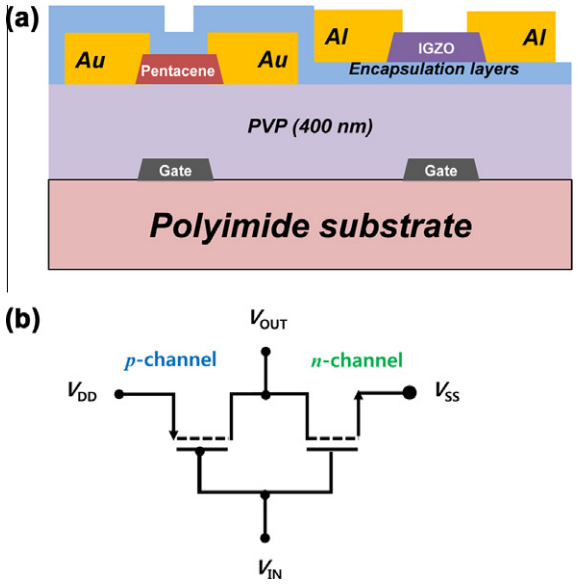

Fig. 1. (a) A schematic diagram of a flexible complementary inverter based on p-channel pentacene and n-channel IGZO TFTs. (b) A diagram of a complementary inverter circuit.

The basic electrical characteristics of individual TFTs and circuits were monitored by a semiconductor parameter analyzer (HP4145B, Agilent Technologies) at room temperature in the dark. The performances of TFTs and circuits under mechanical deformation were then measured. The voltage transfer characteristics (V_{OUT}–V_{IN}) and DC voltage gain ($-dV_{OUT}/dV_{IN}$) of flexible inverter circuits were evaluated and the effects of mechanical bending on their performance, such as shifts of the switching threshold voltage, were also analyzed.

3. Electrical analysis of flexible devices under mechanical deformation

Fig. 2(a) shows the changes in the characteristics of an as-fabricated p-cannel pentacene TFT in the saturation region at different bending radii causing tensile strain. The transfer characteristics of p-channel TFTs in the saturation region were obtained by applying a gate voltage (V_G) that is swept from 10 V to −20 V while maintaining a source–drain voltage (V_{SD}) of −20 V. According to the initial transfer characteristics, the current on–off ratio (I_{on}/I_{off}) is about

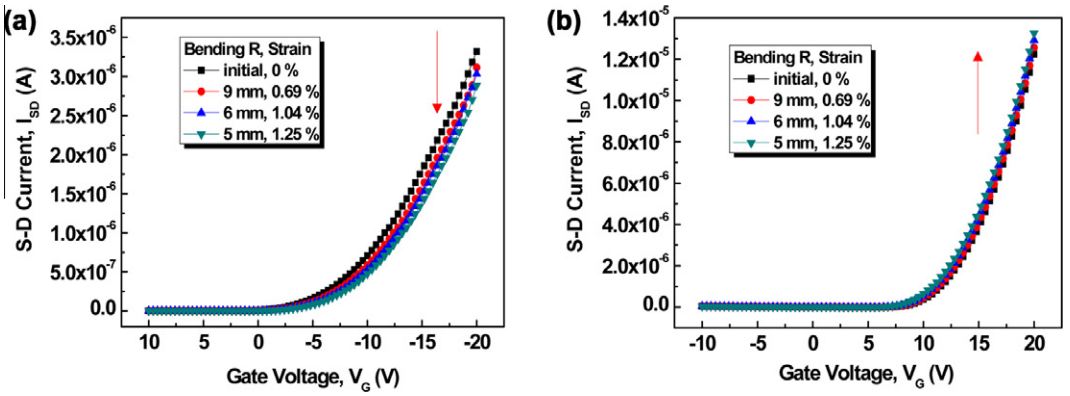

Fig. 2. The transfer characteristics in the saturation regions of TFTs at different bending radii. (a) The p-channel transfer characteristics of the pentacene TFT with the applied gate bias (V_G) ranging from 10 V to −20 V while maintaining the source–drain voltage (V_{SD}) at −20 V. (b) The n-channel transfer characteristics of an n-channel TFT obtained by sweeping V_G from −10 V to 20 V while maintaining V_{SD} at 20 V.

10^3 (not shown). The field-effect channel mobility in the saturation region ($\mu_{sat,p}$) and the threshold voltage (V_{tp}) were also calculated as 0.6 cm^2/V s and −1.5 V, respectively. The saturated source–drain current decreased as the bending radius was decreased. This phenomenon might be explained by two possible reasons. One is the change of the charge transport properties of the molecular pentacene. Charge transport in pentacene is directly related to the hole hopping rate which is inversely proportional to the distance between hopping sites [24]. Hence, the reason why the saturated source–drain current decreased under tensile strain is that larger spacing between pentacene molecules causes a decrease of hole mobility and, in turn, conductivity. On the other hand, another possible reason is change of surface energy and heterogeneity of the interface between a dielectric and a semiconductor. A recent report has investigated that the device mobility is changed under the mechanical deformation due to rearrangement of polymer structure at the surface on the dielectric layer [25]. In tensile strain, therefore, local reorientation of polymer chains may be able to change the carrier mobility and the channel current.

The transfer characteristics of n-channel IGZO TFTs in the saturation region were also measured while decreasing the bending radius, as shown in Fig. 2(b). The V_G was swept from −10 V to 20 V while applying a V_{SD} of 20 V. Before bending, the I_{on}/I_{off} value was about 10^4 (not shown). The field-effect channel mobility in the saturation region ($\mu_{sat,n}$) and the threshold voltage (V_{tn}) were also calculated as 3.6 cm^2/V s and −8.4 V, respectively. In the case of IGZO TFTs, the source–drain saturation current increased under tensile strain. There are two possible factors that could explain these phenomena. One is the doping effect in the IGZO active layer. As previously reported, the charge transport of oxide semiconductors is related to the generation of carriers caused by native defects such as oxygen vacancies during the process [26–28]. Thus the applied tensile strain might affect O vacancies which could change the electron concentration under mechanical deformation. As previously reported in the literature [29], on the other hand, the mobility increase for tensile strain can be possibly correlated with a decrease in the effective mass of electrons due to decreased energy spacing in the direction parallel to the current flow. More detailed study is required to elucidate mechanism of changes in field-effect channel mobility and threshold voltage in organic as well as oxide TFTs.

Fig. 3(a) and (b) show the changes in the parameters of each TFT under tensile strain. We estimated the field-effect mobility by using the equation $I_{SD} = (\mu_{sat}C/2)(W/L)(V_G - V_t)^2$ in the saturation region, where C is the gate dielectric capacitance, W is the channel width, and L is the channel length. In the case of pentacene TFTs, as shown in Fig. 3(a), $\mu_{sat,p}$ decreased and V_{tp} increased when the bending radius was decreased. In contrast, the change in $\mu_{sat,n}$ of the IGZO TFT under tensile strain showed the opposite tendency to that of $\mu_{sat,p}$ of the pentacene TFT with increasing bending radius (see Fig. 3(b)). As mentioned above, the results, which were extracted from the bending experiment, might be related to the different changes in device performance under mechanical bending, which are caused by an increase of hopping rate in organic TFTs and a decrease of the effective mass in oxide TFTs.

Fig. 4(a) and (b) shows the measured voltage transfer characteristics of the hybrid complementary inverters. The switching threshold voltage (V_{th}) and DC voltage gain ($-dV_{OUT}/dV_{IN}$) values with no mechanical bending were estimated to be 11.6 V and 46 V/V at a V_{DD}, drain voltage of a unit circuit, of 20 V, respectively. When the bending radius gradually decreased, the V_{th} was shifted in the negative direction (Fig. 4(a)). On the other hand, the $-dV_{OUT}/dV_{IN}$, which is directly related to the subthreshold swing (S) of each TFT showed no clear trend with decreasing bending radius (Fig. 4(b)). Even though the S values were evaluated and compared, there was also no apparent tendency in the S with bending radius (not shown here). Further studies may be required to achieve a deeper understanding of the effects of mechanical deformation on the DC voltage gains of complementary inverters.

In the general theory, the field-effect mobility and threshold voltage of p- and n-channel TFTs are important parameters that determine the V_{th} of a complementary inverter, which is given by the following equation:

$$V_{th} = \frac{r(V_{DD} + V_{tp}) + V_{tn}}{1 + r}, \quad (1)$$

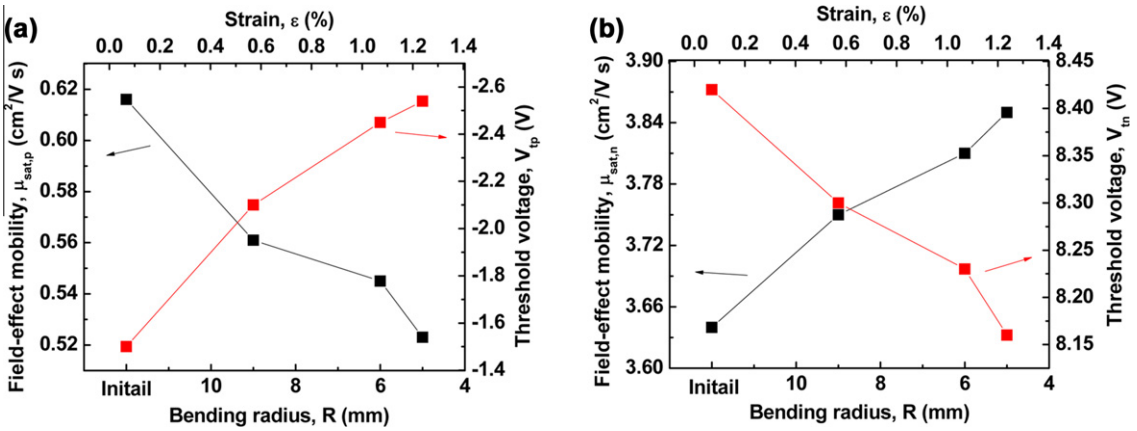

Fig. 3. The changes in field-effect mobility (black line) and threshold voltage (red line) of (a) the p-channel pentacene TFT and (b) the n-channel IGZO TFT under mechanical deformation. (For interpretation of the references to color in this figure legend, the reader is referred to the web version of this article.)

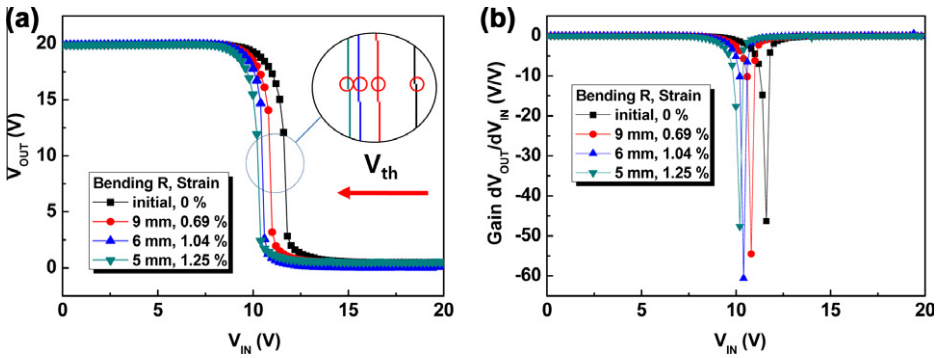

Fig. 4. (a) Voltage transfer characteristics of the flexible complementary inverter at V_{DD} = 20 V and (b) the obtained voltage gain values for different bending radii. As the bending radius decreased, the V_{th} value shifted in the negative direction; the voltage gain value increased as the bending radius decreased down to 6 mm and then slightly decreased at the bending radius of 5 mm.

Here, the r factor is given by:

$$r = \sqrt{\frac{\mu_{sat,p}(W_p/L_p)}{\mu_{sat,n}(W_n/L_n)}}, \tag{2}$$

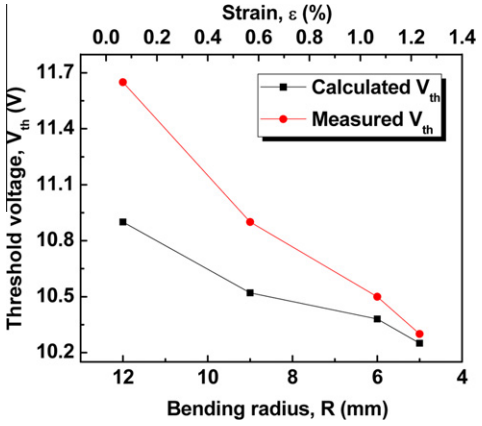

Fig. 5. Calculated and measured V_{th} values of the flexible complementary inverters for different bending radii.

where W_n and W_p are the channel widths and L_n and L_p are the channel lengths of the n- and p-channel TFTs, respectively. We can evaluate expected phenomena such as shifts of V_{th} in the fabricated inverters by using Eq. (1). The calculated and measured V_{th} values are shown in Fig. 5. As expected from Eq. (2), the r factor decreases with decreasing bending radius, which leads to a decrease of V_{th}. According to Eq. (1), moreover, the increase of the difference between V_{tp} and V_{tn} also brings about a shift of V_{th} in the negative direction. Even though there are some discrepancies in the calculated and measured values, the tendency in the measured V_{th} variation with bending radius agrees well with that from the theoretical estimations using Eq. (1).

4. Conclusion

In this work, we have investigated the relationship between the electrical characteristics of TFTs and the performance changes in complementary inverters under mechanical deformation. In the case of TFTs, changes in field-effect mobility and threshold voltage were observed with opposite tendencies for n-channel and p-channel de-

vices, which also affected the shift of voltage transfer characteristics in flexible inverters. The results indicate the importance of understanding the performance changes in component devices in order to elucidate the changes in flexible circuits upon mechanical deformation.

Acknowledgment

This work was supported by the IT Research and Development program of MKE/KEIT (KI002182, TFT backplane technology for next generation displays).

References

[1] J.B. Kim, C. Fuentes-Hernandez, D.K. Hwang, W.J. Potscavage Jr., H. Cheun, B. Kippelen, Org. Electron. 12 (2011) 45.
[2] P.T. Liu, Y.T. Chou, L.F. Teng, C.S. Fuh, Appl. Phys. Lett. 97 (2010) 083505.
[3] J.H. Na, M. Kitamura, Y. Arakawa, Appl. Phys. Lett. 93 (2008) 213505.
[4] J.B. Kim, C. Fuentes-Hernandez, S.J. Kim, S. Choi, B. Kippelen, Org. Electron. 11 (2010) 1074.
[5] M.S. Oh, W.J. Choi, K.M. Lee, D.K. Hwang, S.I. Im, Appl. Phys. Lett. 93 (2008) 033510.
[6] A. Dodabalapur, J. Baumback, K. Baldwin, H.E. Katz, Appl. Phys. Lett. 68 (1996) 2246.
[7] Y. Chen, S. Wagner, Appl. Phys. Lett. 75 (1999) 1125.
[8] R.B. Min, S. Wagner, Appl. Phys. A 74 (2002) 541.
[9] P.I. Hsu, R. Bhattacharya, H. Gleskova, M. Huang, Z. Xi, Z. Suo, S. Wagner, J.C. Sturm, Appl. Phys. Lett. 81 (2002) 1723.
[10] T. Shimoda, Y. Matsuki, M. Furusawa, T. Aoki, I. Yudasaka, H. Tanaka, H. Iwasawa, D. Wang, M. Miyasaka, Y. Takeuchi, Nature 440 (2006) 783.
[11] G.H. Gelinck, H. Edzer, A. Huitema, E. van Veenendaal, E. Cantatore, L. Schrijnemakers, J.B.P.H. van der Putten, T.C.T. Geuns, M. Beenhakkers, J.B. Giesbers, B. Huisman, E.J. Meijer, E.M. Benito, F.J. Touwslager, A.W. Marsman, B.J.E. van Rens, D.M. de Leeuw, Nat. Mater. 3 (2004) 106.
[12] S.R. Forrest, Nature 428 (2004) 911.
[13] V. Subramanian, P.C. Chang, J.B. Lee, S.E. Molesa, S.K. Volkman, IEEE Trans. Compon. Packag. Technol. 28 (2005) 742.
[14] H. Sirringhaus, T. Kawase, R.H. Friend, T. Shimoda, M. Inbasekaran, W. Wu, E.P. Woo, Science 290 (2000) 2123.
[15] W.C. Shin, H. Moon, S.H. Yoo, Y. Li, B.J. Cho, IEEE Electron. Device Lett. 31 (2010) 1308.
[16] L.S. Hung, C.H. Chen, Mater. Sci. Eng. R 39 (2002) 143.
[17] T. Sekitani, Y. Kato, S. Iba, H. Shinaoka, T. Someya, T. Sakurai, S. Takagi, Appl. Phys. Lett. 86 (2005) 073511.
[18] Y.G. Seol, N.-E. Lee, S.H. Park, J.Y. Bae, Org. Electron. 9 (2008) 413.
[19] K.S. Sim, Y.I. Choi, H.J. Kim, S.W. Cho, S.C. Yoon, S.M. Pyo, Org. Electron. 10 (2009) 506.
[20] P. Liu, Y. Wu, Y. Li, B.S. Ong, S. Zhu, J. Am. Chem. Soc. 128 (2006) 4554.
[21] Z. Bao, A.J. Lovinger, J. Brown, J. Am. Chem. Soc. 120 (1998) 207.
[22] Y. Hosoi, D. Tsunami, H. Ishii, Y. Furukawa, Chem. Phys. Lett. 436 (2007) 139.
[23] T. Sekitani, U. Zschieschang, H. Klauk, T. Someya, Nat. Mater. 9 (2010) 1015.
[24] V. Ambegaokar, B.I. Halperin, J.S. Langer, Phys. Rev. B 4 (1971) 2612.
[25] A.N. Sokolov, Y. Cao, O.B. Johnson, Z. Bao, Adv. Funct. Mater. 22 (2012) 175.
[26] A.F. Kohan, G. Ceder, D. Morgan, C.G. Van de Walle, Phys. Rev. B 61 (2000) 15019.
[27] D.C. Look, G.C. Farlow, P. Reunchan, S. Limpijumnong, S.B. Zhang, K. Nordlund, Phys. Rev. Lett. 95 (2005) 225502.
[28] Y.S. Kim, C.H. Park, Phys. Rev. Lett. 102 (2009) 086403.
[29] N. Münzenrieder, K.H. Cherenack, IEEE Trans. Electron. Device 58 (2011) 2041.